

MANGROVE: Mapping and Analyzing the Geomorphological Roles of Mangrove Vegetation and its contribution to erosion control for sustainable coastal development in Baganga, Davao Oriental

*Frences Ann B. Villamor, Keith Joshua M. Ayag, Paulene Beatriz D. Tabirara, John Ritzzy C. Buenaflor, Christine Mae N. Corcino, Louise Angelique Rose C. Babas, and Christian Paul F. Escarian**

University of Southeastern Philippines, BS in Geology Program, Davao City, Philippines

Abstract. Coastal geomorphology in typhoon-prone regions of the Philippines is increasingly threatened by erosion and shoreline retreat, compounded by population growth, anthropogenic pressures, and the degradation of mangrove ecosystems. Mangrove forests, due to their sediment-trapping capacity and wave attenuation function, serve as natural buffers that enhance shoreline stability. This study assesses the geomorphological role of mangroves in mitigating coastal erosion along the shoreline of Baganga, Davao Oriental. Multi-temporal satellite imagery from 2000 to 2025 was analyzed to quantify changes in mangrove distribution and shoreline position. Mangrove coverage was mapped using the Post-Classification Change Detection, which works by carefully comparing each image pixel by pixel to detect changes in land cover types, such as mangroves, across different layers, often requiring the classifications to be resampled to a common resolution and grid to ensure accurate comparisons. Shoreline dynamics were assessed using the Digital Shoreline Analysis System (DSAS), applying Net Shoreline Movement (NSM), End Point Rate (EPR), and Linear Regression Rate (LRR) to evaluate patterns of erosion and accretion.

1 Introduction

The Municipality of Baganga, located along the eastern portion of Davao Oriental, was observed to have an increased from 56,242 in 2015 to 58,714 in 2020, with many settlements expanding into coastal zones identified as highly susceptible to natural hazards. Notably, this exposure was catastrophically underscored in 2012 when Super Typhoon Pablo (internationally known as “Bopha”) devastated the region as a Category 5 storm. The event destroyed approximately 200,000 homes, caused over 1,000 fatalities,

* Corresponding author: cpfescarian@usep.edu.ph

and inflicted damages exceeding US\$1 billion [1]. Conversely, the loss of mangrove forests during this period significantly weakened Baganga's natural coastal defenses.

Mangroves serve as bio-geomorphic buffers, reducing wave energy and trapping sediments to maintain shoreline equilibrium [2]. Despite their ecological importance, Philippine mangroves continue to decline due to land conversion, overharvesting, and recurrent typhoons [3-4]. This degradation increases the rate of coastal erosion and habitat fragmentation. The study draws upon the Ecosystem Services Theory of Costanza and others (1997) [5], which frames mangroves as providers of regulating and supporting ecosystem services essential for community resilience. Accordingly, the study hypothesizes that denser mangrove stands correspond to higher rates of shoreline accretion due to enhanced sediment retention and root stabilization effects.

By quantifying the relationship between mangrove cover and shoreline dynamics, this research contributes to regional strategies for sustainable coastal development. The findings provide actionable data for local governments and environmental planners seeking to design coastal protection programs that integrate natural ecosystem functions with engineering solutions.

2 Materials and Methods

Mangrove distribution data were obtained from UNEP-WCMC global mangrove layers, while shoreline positions were derived from Landsat 4-5 TM, Landsat 7 ETM+, and Sentinel-2A MSI imagery covering 2000–2025 (*see Table 1*). Imagery was filtered to maintain <30% cloud cover and pre-processed using ENVI 5.3 and SNAP 7.0 software for geometric alignment and atmospheric correction. Sentinel-2 images were further processed to Bottom-of-Atmosphere reflectance using the Sen2Cor plugin.

The Normalized Difference Water Index (NDWI) was calculated to delineate land-water interfaces using the formula:

$$NDWI = \frac{B_{GREEN} - B_{NIR}}{B_{GREEN} + B_{NIR}} \quad (1)$$

where B_{Green} and B_{NIR} correspond to the green and near-infrared bands, respectively. Positive NDWI values indicated water bodies, while negative values corresponded to land. The classified images underwent K-Means clustering to refine feature boundaries, ensuring accurate extraction of shoreline positions across time intervals.

Mangrove cover change was determined using the Post-Classification Change Detection method, allowing pixel-by-pixel comparison across timeframes (2007–2010, 2010–2015, 2015–2020). This approach minimized atmospheric and illumination inconsistencies by standardizing datasets to a common resolution and coordinate grid [6]. The resulting maps visualized gains (green) and losses (red) in mangrove canopy coverage.

Shoreline vectors were processed in the Digital Shoreline Analysis System (DSAS) v5.0 to compute NSM, SCE, EPR, and LRR indices. Baselines were generated landward of the coast, with transects spaced every 10 meters. The absence of a local tide gauge was

addressed by using Tandag’s RLR data as a proxy due to similar geomorphic conditions along the Pacific Coast[7]. This ensured consistent sea-level referencing across datasets.

The study applied Spearman’s rank correlation to examine relationships between mangrove cover change and shoreline movement (EPR). The analysis was conducted using SPSS, with correlation coefficients interpreted according to conventional strength thresholds. Shown in Figure 1 is the general workflow of the study.

Table 1. Satellite Images Used for Mangrove Analysis, Including Acquisition Dates, Spatial Resolution, and Cloud Cover from 2000 to 2025.

Year	Satellite	Acquisition Date	Resolution (m)	Cloud Cover (%)	Water Level (m)
2000	Landsat 4-5 TM	2000/04/13	30	14	6.915
2005	Landsat 7 ETM+	2005/10/07	30	18	6.973
2010	Landsat 7 ETM+	2010/03/05	30	12	7.030
2015	Sentinel 2-A L1C	2015/11/21	10	21	6.961
2020	Sentinel 2-B L2A	2020/09/25	10	6	7.060
2025	Sentinel 2-B L2A	2025/01/17	10	15	6.983

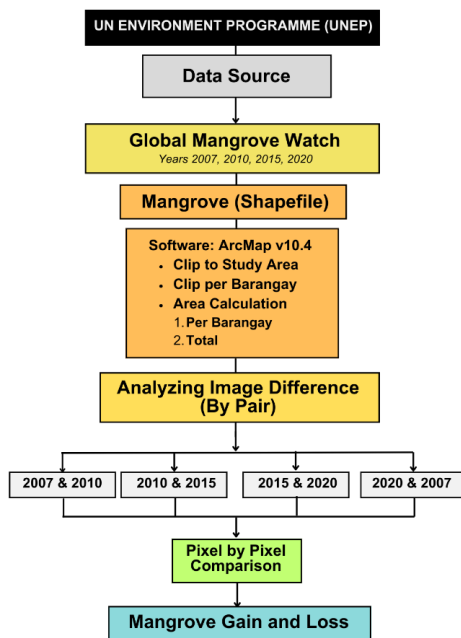


Fig. 1. Workflow of Mangrove Mapping Using Post-Classification Change Detection.

3 Results and Discussion

3.1 Mangrove Distribution and Change

Spatial analysis revealed that mangrove canopies were predominantly located in Barangays Bobonao, Salingcomot, and Banao, forming continuous estuarine forests. Bobonao exhibited the largest extent (4.51 sq. km), followed by Salingcomot (2.99 sq. km) and Banao (2.86 sq. km). Meanwhile, Central, Baculin, and Kinablangan showed moderate coverage, whereas Dapnan and Lambajon lacked notable mangrove presence.

Temporal analysis indicated that between 2007 and 2020, Central experienced the greatest increase in mangrove cover (+4.02%), while San Victor suffered the highest loss (-12.16%) (see Table 2). These results highlight spatial disparities in ecosystem resilience, likely influenced by local geomorphology and hydrological connectivity.

Table 2. Mangrove cover area and percentage change by Barangay from 2007 to 2020, showing trends across three time periods and overall net change.

Barangay	Area (sq. km)	2007-2010	2010-2015	2015-2020	2007-2020
Baculin	0.74	0.34%	-0.60%	2.29%	2.03%
Bobonao	4.51	-0.80%	-0.02%	0.40%	-0.43%
Salingcomot	2.99	-0.09%	-0.16%	-0.09%	-0.34%
Central	1.38	-7.03%	0.43%	11.41%	4.02%
San Victor	0.43	6.32%	-9.74%	-8.47%	-12.16%
Kinablangan	0.55	-2.28%	0.44%	-1.28%	-3.10%
Banao	2.86	0.13%	-0.56%	-0.89%	-1.33%

The DSAS analysis revealed heterogeneous shoreline behavior. Central exhibited the highest accretion (NSM = 87.54 m; EPR = 1.39 m/yr), correlating with increased mangrove density. Dapnan, despite lacking mangroves, recorded substantial accretion (72.63 m), likely influenced by sediment deposition from fluvial sources. Conversely, Baculin (-12.66 m) and Kinablangan (-16.72 m) experienced significant erosion, consistent with reduced vegetative buffering (see Table 3 and Figures 2 & 3).

Table 3. Rate of changes (NSM, SCE, EPR, and LRR indexes) of Baganga from 2000-2025.

Barangay	Average Rate			
	NSM (m)	SCE (m)	EPR (m/yr)	LRR (m/yr)
Baculin	-12.66	57.85	-0.5	-1.22
Bobonao	9.44	33.34	0.38	0.78
Salingcomot	11.76	38.83	0.47	0.93
Central	87.54	33.93	1.39	2.15
San Victor	23.2	85.89	0.59	1.47
Kinablangan	-16.72	41.91	-0.67	-1.22
Banao	-5.02	71.28	-0.23	-0.74
Lambajon	12.62	45.28	0.5	1.03
Dapnan	72.63	19.22	0.74	1.36

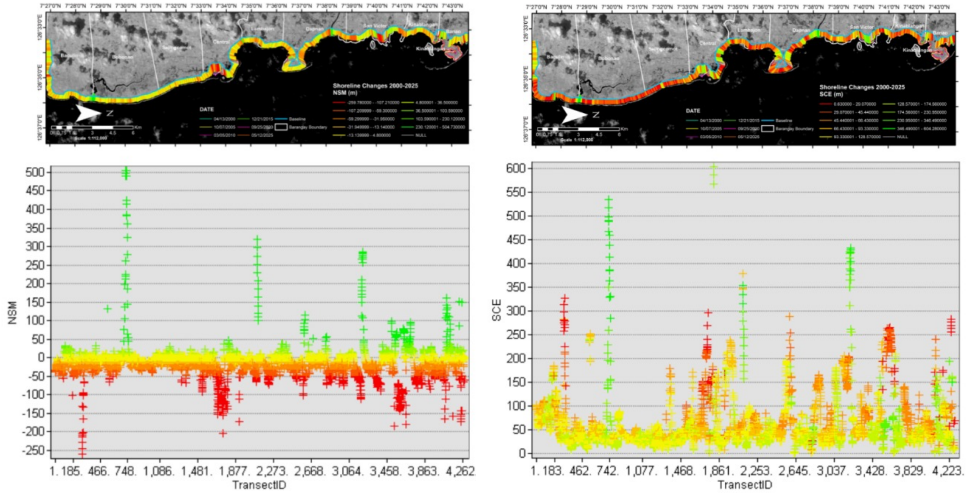


Fig. 2. (a) Shoreline changes (2000-2025) based on net shoreline movement (NSM) and (b) shoreline change envelope (SCE) along Baganga Shoreline.

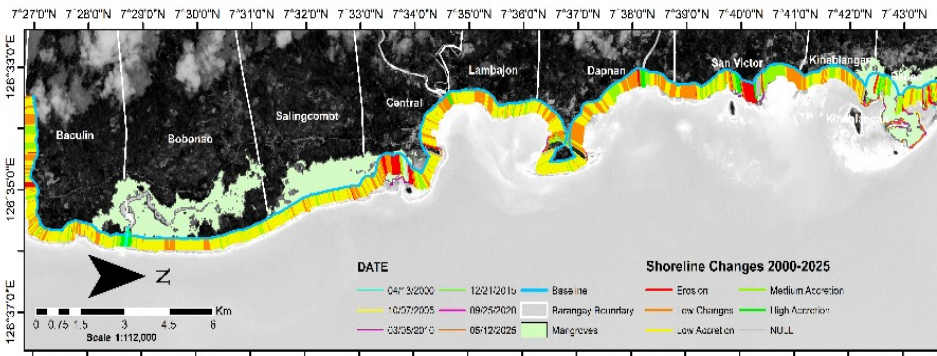


Fig. 3. Shoreline Change Map and Mangrove Cover Distribution Map overlay in the Municipality of Baganga, Davao Oriental.

The Spearman correlation ($r = 0.368$) indicated a weak positive association between mangrove area change and EPR, implying proportional but non-dominant influence. This aligns with global findings suggesting that while mangroves attenuate wave energy, shoreline evolution remains multi-causal [8]. The weak correlation also reflects unmeasured variables such as sediment input from rivers, substrate stability, and anthropogenic modifications.

4 Conclusion

This study demonstrated that mangrove vegetation significantly contributes to shoreline stability, though it is not the sole determinant. The spatial overlap of high mangrove density and positive shoreline accretion, notably in Barangay Central, supports their sediment-trapping function. However, the persistence of accretion in non-mangrove zones like Dapnan underscores the role of hydrodynamic and fluvial processes. The

observed weak correlation ($r = 0.368$) suggests that coastal evolution in Baganga is shaped by a complex interplay of biophysical and anthropogenic factors. Future studies should integrate high-resolution topographic data and field-based validation to strengthen predictive models of coastal change. Policymakers are urged to adopt ecosystem-based coastal management strategies that integrate mangrove rehabilitation with engineering interventions to enhance resilience against erosion and sea-level rise.

References

1. H. Pislán, H. Macombo, J. Macombo, Assessment of mangroves affected by Super Typhoon Pablo in Barangay Lucod, Baganga, Davao Oriental. *Davao Res. J.* **12**, 39–55 (2021). <https://doi.org/10.59120/drj.v12i5.74>
2. S. Dasgupta, M. S. Islam, M. Huq, Z. Huque Khan, M. R. Hasib, Quantifying the protective capacity of mangroves from storm surges in coastal Bangladesh. *PLOS ONE.* **14**, e0214079 (2019). <https://doi.org/10.1371/journal.pone.0214079>
3. M. Buitre, H. Zhang, H. Lin, Mangrove forest change and impacts from tropical cyclones in the Philippines using time-series satellite imagery. *Remote Sens.* **11**, 688 (2019). <https://doi.org/10.3390/rs11060688>
4. K. Garcia, D. Gevaña, P. Malabrigo, Philippines' Mangrove Ecosystem: Status, Threats and Conservation. In: Faridah-Hanum, I., Latiff, A., Hakeem, K., Ozturk, M. (eds) *Mangrove Ecosystems of Asia*, (Springer, New York, 2013) https://doi.org/10.1007/978-1-4614-8582-7_5
5. R. Costanza, R. d'Arge, R. de Groot, S. Farber, M. Grasso, B. Hannon, et al., The value of the world's ecosystem services and natural capital. *Nature.* **387**, 253–260 (1997). <https://doi.org/10.1038/387253a0>
6. R. R. Colditz, J. Acosta-Velázquez, J. R. D. Gallegos, A. D. V. Lule, M. T. Rodríguez-Zúñiga, P. Maeda, et al., Potential effects in multi-resolution post-classification change detection. *Int. J. Remote Sens.* **33**, 6426–6445 (2012). <https://doi.org/10.1080/01431161.2012.688148>
7. Alaska Div. Geol. Geophys. Surv., Alaska tidal datum frequently asked questions. Alaska.gov (2023). <https://dggs.alaska.gov/hazards/coastal/ak-tidal-datum-faq.html>
8. S. Thakur, I. Mondal, S. Bar, S. Nandi, P. B. Ghosh, P. Das, T. K. De, Shoreline changes and their impact on mangrove ecosystems of the Indian Sundarbans. *J. Clean. Prod.* **284**, 124764 (2021). <https://doi.org/10.1016/j.jclepro.2020.124764>